A DFT analysis of the relationships between electronic structure and inhibition of aurora kinase A and epidermal growth factor receptor kinase by a set of N[4]-phenyl substituted-7H-pyrrolo[2,3-d]pyrimidin-4-amines

Juan S. Gómez-Jeria*, Vicente Contreras-Lira

Quantum Pharmacology Unit, Department of Chemistry, Faculty of Sciences, University of Chile. Las Palmeras 3425, Santiago 7800003, Chile
J.S. Gómez-Jeria: facien03@uchile.cl

Abstract A quantum-chemical structure-activity study is carried out for the inhibition of aurora kinase A and epidermal growth factor receptor kinase by a group of N[4]-phenylsubstituted-7H-pyrrolo[2,3-d]pyrimidin-4-amines. The Klopman-Peradejordi-Gómez method was employed. Statistically significant relationships between the variation of the inhibitory capacity of a group of N[4]-phenylsubstituted-7H-pyrrolo[2,3-d]pyrimidin-4-amines against aurora kinase A and epidermal growth factor receptor kinase and the variation of the values of several local atomic reactivity indices were obtained. The results are presented in the form of a partial pharmacophore that could be useful in the synthesis of new and more powerful molecules.

Introduction

Cancer is a group of diseases involving uncontrolled cell proliferation occurs in body. Antimitotic molecules, which disrupted mitotic spindle assembly, are usually used to treat almost all kinds of cancer. Kinase inhibitors play a critical role in creation of anti-cancer agents. Common targets for this strategy are Aurora kinase and Polo like kinase. Aurora kinase was identified in 1995 and is a member of the enzymes serine/threonine kinase family. It is involved in G2/M phase of the cell cycle and its regulation process is observed during the complete cell cycle. For more detailed information, see for example the review of Borisa and Bhatt [1]. Dysfunctional epidermal growth factor receptor kinase plays a role in tumor progression and angiogenesis in squamous cell carcinoma of the head and neck, non-small cell lung cancer and colorectal cancer[2]. Given the importance of these kinases for combating cancer, many chemical compounds have been synthesized and tested for inhibitory capacity [2-14].

Recently Kurup et al. published data about the inhibition of aurora kinase A (AURKA) and epidermal growth factor receptor kinase (EGFR) by a group of *N*[4]-phenylsubstituted-7*H*-pyrrolo[2,3-*d*]pyrimidin-4-amines [2]. In this paper we present the results of the application of the Klopman-Peradejordi- Gómez method for the search of relationships between electronic structure and inhibitory capacities of the abovementioned molecules.

Methods and Models

The Klopman-Peradejordi-Gómez (KPG) method belongs to the class of model-based methods. Since this model has been presented in several papers [15-25], we shall present here only its main lines of development and discuss below

only the results obtained here. Starting from the statistical-mechanical definition of the equilibrium constant, an expression relating this experimental value with several local atomic reactivity indices and orientational parameters was developed. Its application to several different molecules and receptors gave very good results (see [23, 26-43] and references therein). Its extension to all kinds of biological activities was very fruitful (see [40, 44-61] and references therein).

The molecules and inhibitory data against AURKA and EGFR were taken from a recent publication, and are presented in Fig. 1 and Table 1.
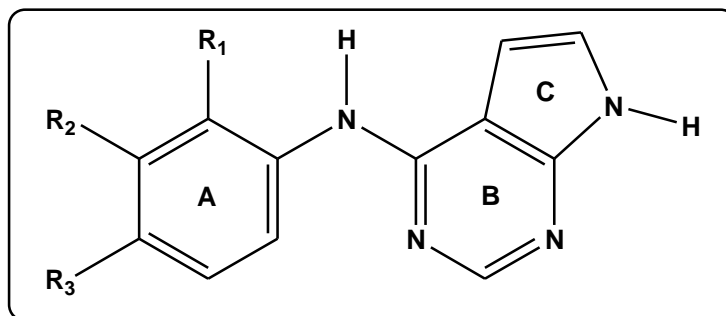

Figure 1: General formula of molecules used in this study

Table 1.

Mol.	R_1	R_2	R_3	$\log(IC_{50})$ AURKA	$\log(IC_{50})$ EGFR
1	H	H	H	0.75	2.41
2	H	Br	H	0.30	0.58
3	H	F	Cl	0.52	0.78
4	H	H	Cl	0.71	1.93
5	H	Cl	Cl	0.59	0.83
6	H	H	OMe	0.83	3.47
7	H	Br	Cl	0.51	0.56
8	H	H	Me	0.74	2.82
9	H	H	Br	0.71	2.10
10	H	Me	H	0.54	1.30
11	H	CF_3	H	0.76	1.64
12	Cl	H	H	0.75	2.67
13	Me	H	H	0.93	3.09
14	H	H	Ph	1.87	----
15	H	H	OPh	1.12	2.05
16	H	H	CH_2Ph	0.70	1.80

Calculations

The electronic structure of all molecules was calculated within the Density Functional Theory (DFT) at the B3LYP/6-31G(d,p) level with full geometry optimization [62]. The Gaussian suite of programs was used [63]. The information needed to calculate the numerical values for the LARIs was obtained from the Gaussian results with the D-Cent-QSAR software [64]. All the electron populations smaller than or equal to 0.01 e were considered as zero. Negative electron populations coming from Mulliken Population Analysis [65] were corrected as usual [66]. Orientational parameters taken from published Tables or calculated in our Unit with the Steric software [67]. Since the resolution of the system of linear equations is not possible because we have not experimental data, we employed Linear Multiple Regression Analysis (LMRA) techniques to find the best solution. For each case, a matrix containing the dependent variable ($\log(IC_{50})$ in this case) and the local atomic reactivity indices of all atoms of the common skeleton as independent variables was built. Regarding the local atomic reactivity indices depending on the MO (Fukui indices and superdelocalizabilities) we have employed only those associated with the frontier local molecular orbitals. The Statistica software was used for LMRA [68].
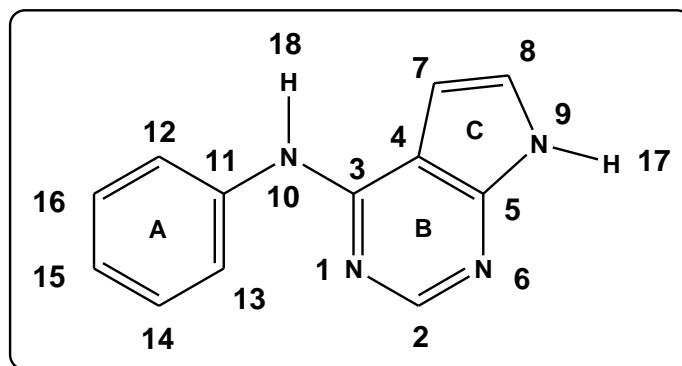
Figure 2: Common skeleton numbering

Results

An initial analysis of the common skeleton

Using the actual knowledge about molecular interactions, we can carry out a previous analysis of the common skeleton to propose several possible interactions. Figure 3 shows the main possible drug-site interactions. We may add C-H...π, lone pair...π and S...π interactions (Gómez-Jeria et al., unpublished). KPG method, in its statistical form, should confirm one or more of them.
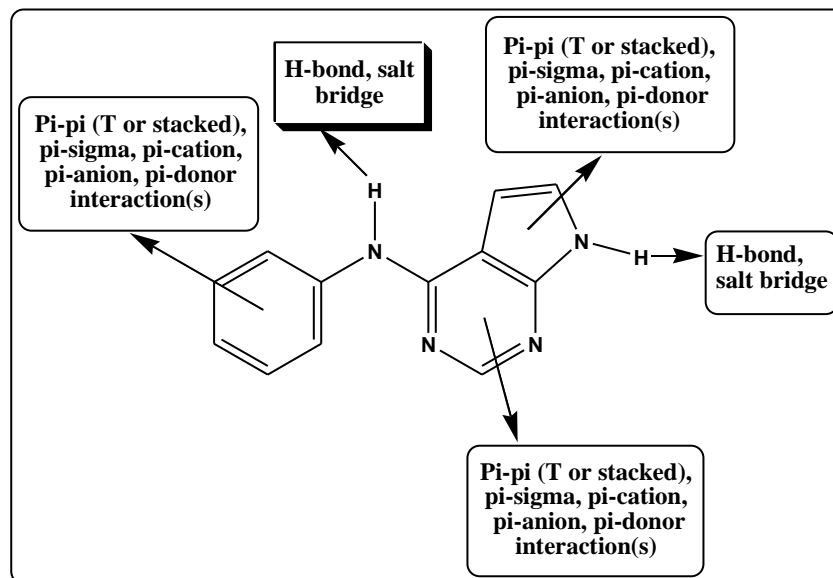

Figure 3: Possible common skeleton-site interactions

Results for aurora kinase A inhibition (AURKA)

The best statistically significant equation obtained is the following:

$$\log(IC_{50}) = 1.32 - 2.76F_7(LUMO+2)^* + 1.81F_7(HOMO-1)^* \tag{1}$$

with n=16, R=0.97, R^2=0.94, adj-R^2=0.93, f(2,13)=102.7 (p<0.000001) and a standard error of the estimate of 0.09. No outliers were detected and no residuals fall outside the ±2σ limits. Here, $F_7(LUMO+2)^*$ is the Fukui index of the third lowest empty MO localized on atom 7 and $F_7(HOMO-1)^*$ is the Fukui index of the second highest occupied MO localized on atom 7. Tables 2 and 3 show, respectively, the beta coefficients, the results of the t-test for significance of coefficients and the matrix of squared correlation coefficients for the variables of Eq. 1. There are no significant internal correlations between independent variables (Table 3). Figure 3 displays the plot of observed *vs.* calculated $\log(IC_{50})$.

Table 2: Beta coefficients and t-test for significance of coefficients in Eq. 1

	Beta	t(13)	p-level
F$_7$(LUMO+2)*	-1.10	-14.20	<0.000001
F$_7$(HOMO-1)*	0.41	5.30	<0.0001

Table 3: Matrix of squared correlation coefficients for the variables in Eq. 1

	F$_7$(LUMO+2)*	F$_7$(HOMO-1)*
F$_7$(LUMO+2)*	1.00	
F$_7$(HOMO-1)*	0.24	1.00

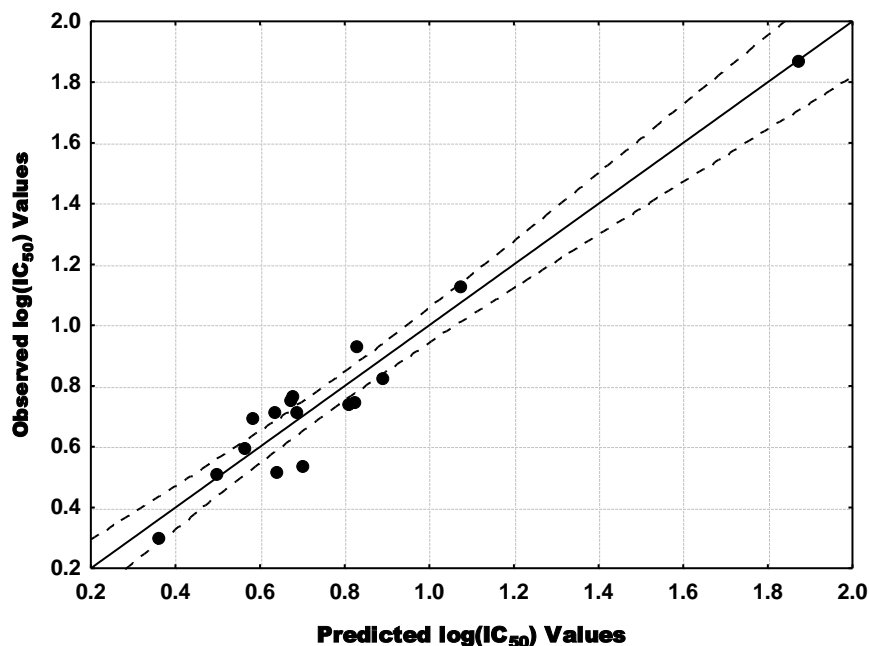*Figure 4: Plot of predicted vs. observed log(IC$_{50}$) values (Eq. 1). Dashed lines denote the 95% confidence interval*
The associated statistical parameters of Eq. 1 indicate that this equation is statistically significant and that the variation of the numerical values of a group of two local atomic reactivity indices of atoms of the common skeleton explains about 93% of the variation of log(IC$_{50}$). Figure 4, spanning about 1.6 orders of magnitude, shows that there is a good correlation of observed *versus* calculated values.

Results for epidermal growth factor receptor kinase inhibition (EGFR)
The best statistically significant equation obtained is the following:

$$\log(IC_{50}) = -10.03 - 6.90 S_{12}^{E}(HOMO)* - 7.77 S_{3}^{E}(HOMO-2)* + $$
$$+4.38 F_9(LUMO+2)* + 15.38 Q_{11}$$

(2)

with n=14, R=0.99, R^2=0.98, adj-R^2=0.98, F(4,9)= 191.06 (p< 0.00000x) and a standard error of estimate of 0.12. No outliers were detected and no residuals fall outside the ±2σ limits. Here, S$_{12}^{E}$(HOMO)* is the electrophilic superdelocalizability of the highest occupied MO localized on atom 12, S$_3^{E}$(HOMO-2)* is the electrophilic superdelocalizability of the third highest occupied MO localized on atom 3, F$_9$(LUMO+2)* is the Fukui index of the third lowest empty MO localized on atom 9 and Q$_{11}$ is the net charge of atom 11. Tables 4 and 5 show, respectively, the beta coefficients, the results of the t-test for significance of coefficients and the matrix of squared correlation coefficients for the variables of Eq. 2. There are no significant internal correlations between independent variables (Table 4). Figure 5 displays the plot of observed *vs.* calculated log(IC$_{50}$).

Table 4: Beta coefficients and t-test for significance of coefficients in Eq. 2

	Beta	**t(9)**	**p-level**
$S_{12}^E(HOMO)^*$	-0.87	-21.06	<0.000001
$S_3^E(HOMO-2)^*$	-0.53	-14.31	<0.000001
$F_9(LUMO+2)^*$	0.22	5.65	<0.0003
Q_{11}	0.17	4.24	<0.002

Table 5: Matrix of squared correlation coefficients for the variables in Eq. 2

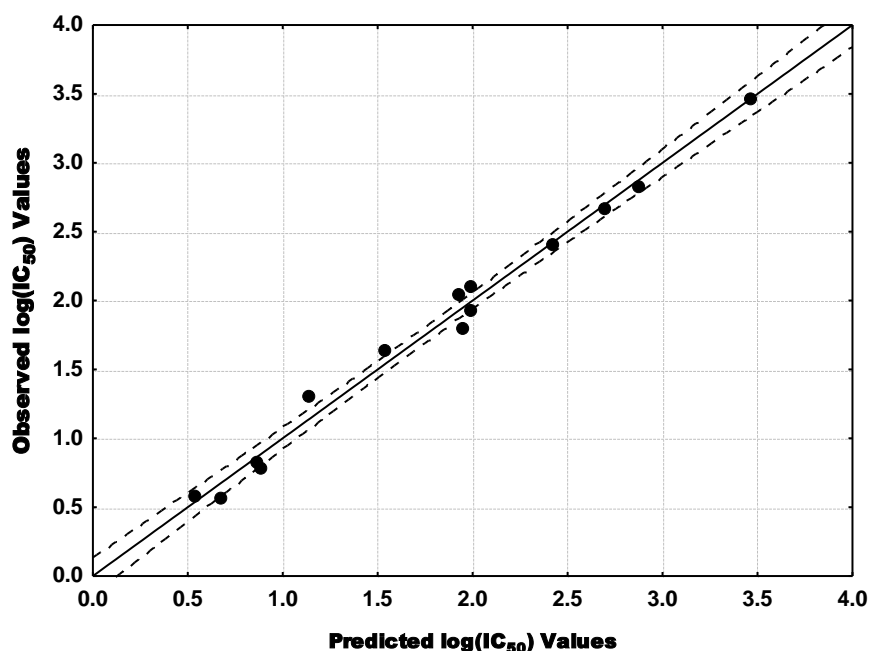|	$S_{12}^E(HOMO)^*$	$S_3^E(HOMO-2)^*$	$F_9(LUMO+2)^*$	Q_{11}
$S_{12}^E(HOMO)^*$	1.00			
$S_3^E(HOMO-2)^*$	0.01	1.00		
$F_9(LUMO+2)^*$	0.08	0.04	1.00	
Q_{11}	0.12	0.01	0.02	1.00

Figure 5: Plot of predicted vs. observed log(IC$_{50}$) values (Eq. 2). Dashed lines denote the 95% confidence interval

The associated statistical parameters of Eq. 2 indicate that this equation is statistically significant and that the variation of the numerical values of a group of four local atomic reactivity indices of atoms of the common skeleton explains about 98% of the variation of log(IC$_{50}$). Figure 5, spanning about 3 orders of magnitude, shows that there is a good correlation of observed *versus* calculated values. Note that when a local atomic reactivity index of an inner occupied MO (i.e., HOMO-1 and/or HOMO-2) or of a higher vacant MO (LUMO+1 and/or LUMO+2) appears in one equation, it implies that the remaining of the upper occupied MOs (for example, if HOMO-2 appears, upper means HOMO-1 and HOMO) or the remaining of the empty MOs (for example, if LUMO+1 appears, lower means the LUMO) contribute to the interaction. Their nonappearance in the equation only means that the variation of their numerical values is not statistically significant.

Local molecular orbitals
Tables 6 and 7 show the local molecular orbitals of atoms 3, 7, 9, 11 and 12.

Table 6: Local molecular orbitals of atoms 3, 7 and 9

Mol.	3(C)	7(C)	9(N)
1(55)	52σ54π55π-56π57π58π	51π54π55π-56π59π60π	52σ54π55π-56π57π58π
2(72)	70π71π72π-73π77π78π	70π71π72π-73π77π78π	70π71π72π-73π74π75π
3(67)	64σ66π67π-68π70π71π	65π66π67π-68π71π73π	64σ66π67π-68π69π70π
4(63)	61σ62π63π-64π66π67π	59π62π63π-64π67π69π	61σ62π63π-64π65π66π
5(71)	68σ70π71π-72π76π77π	69π70π71π-72π76π77π	68σ70π71π-72π74π76π
6(63)	61σ62π63π-64π65π66π	59π62π63π-64π67π68π	60π61σ62π-64π65π66π
7(80)	77σ79π80π-81π85π86π	78π79π80π-81π85π86π	78π79π80π-81π84π85π
8(59)	56σ58π59π-60π61π62π	55π58π59π-60π63π64π	56σ58π59π-60π61π62π
9(72)	70π71π72π-73π77π78π	68π71π72π-73π77π78π	70σ71π72π-73π74π75π
10(59)	57π58π59π-60π61π62π	57π58π59π-60π63π64π	57π58π59π-60π61π62π
11(71)	69σ70π71π-72π73π75π	68π70π71π-72π75π76π	69σ70π71π-72π74π75π
12(63)	60π62π63π-64π68π69π	61π62π63π-64π68π69π	61π62π63π-64π65π66π
13(59)	56σ58π59π-60π61π62π	57π58π59π-60π63π64π	57π58 π59π-60π61π62π
14(75)	71σ74π75π-76π77π78π	71σ74π75π-76π77π78π	71π74π75π-77π80π81π
15(79)	77π78π79π-80π84π85π	77π78π79π-80π84π85π	77π78π79π-80π82π83π
16(79)	77π78π79π-80π84π85π	77π78π79π-80π85π86π	77π78π79π-80π81π83π

Table 7: Local molecular orbitals of atoms 11 and 12

Mol.	11(C)	12(C)
1(55)	49π54π55π-56π57π58π	53π54π55π-56π57π58π
2(72)	70π71π72π-73π74π75π	70π71π72π-73π74π75π
3(67)	62π66π67π-68π69π70π	59π65π67π-68π69π70π
4(63)	58π62π63π-64π65π66π	60π62π63π-64π65π66π
5(71)	69π70π71π-72π73π74π	64σ69π71π-72π73π75σ
6(63)	60π62π63π-64π65π66π	60π62π63π-64π65π66π
7(80)	78π79π80π-81π82π83σ	75σ78π80π-81π82π83σ
8(59)	54π58π59π-60π61π62π	57π58π59π-60π61π62π
9(72)	64π71π72π-73π74π75π	69π71π72π-73π74π75π
10(59)	57π58π59π-60π61π62π	52σ57π59π-60π61π62π
11(71)	65π70π71π-72π73π74π	68π70π71π-72π73π74π
12(63)	61π62π63π-64π65π66π	61π62π63π-64π65π66π
13(59)	57π58 π59π-60π61π62π	57π58π59π-60π61π62π
14(75)	72π74π75π-76π77π81π	72π73π75π-76 π77π78π
15(79)	77π78π79π-80π81π82π	77π78π79π-80π81π82π
16(79)	77π78π79π-80π81π83π	76π78π79π-80π81π84π

Discussion

Discussion for aurora kinase A inhibition (AURKA)

Table 2 shows that the importance of variables in Eq. 1 is $F_7(LUMO+2)^* \gg F_7(HOMO-1)^*$. A high inhibitory activity is associated with high positive values of $F_7(LUMO+2)^*$ and small positive values of $F_7(HOMO-1)^*$. Table 6 shows that $(HOMO-1)_7^*$, $HOMO_7^*$, $LUMO_7^*$, $(LUMO+1)_7^*$ and $(LUMO+2)_7^*$ have a π nature. Atom 7 is a carbon in ring C (Fig. 2). A high value of $F_7(LUMO+2)^*$ indicates that atom interacts with an electron-rich center in the enzyme. Considering that $F_7(LUMO+1)^*$ and $F_7(LUMO)^*$ should also participate in the interaction, it is possible to speculate that the center could be a carboxylate moiety or an aromatic ring. On the other hand, small positive values of $F_7(HOMO-1)^*$ are needed for better inhibitory activity. This means that $F_7(HOMO-1)^*$ and $F_7(HOMO)^*$ are engaged in a repulsive interaction with occupied MOs of the enzyme, fact that is in agreement with

the requirements for the empty local MOs. All the suggestions are displayed in the partial 2D pharmacophore of Fig. 6.
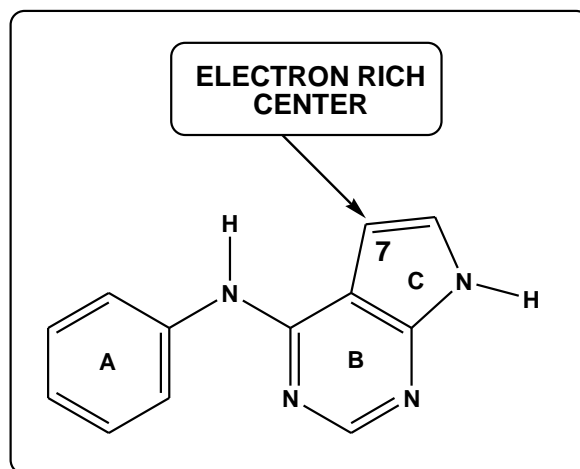

Figure 6: Partial 2D pharmacophore for the inhibition of aurora kinase A by a set of N^4-phenyl substituted-7H-pyrrolo[2,3-d]pyrimidin-4-amines

Discussion for the epidermal growth factor receptor kinase inhibition (EGFR)

Table 4 shows that the importance of variables in Eq. 2 is $S_{12}^E(HOMO)^* > S_3^E(HOMO-2)^* > F_9(LUMO+2)^* > Q_{11}$. A high inhibitory activity is associated with small (negative) values for $S_{12}^E(HOMO)^*$ and $S_3^E(HOMO-2)^*$, with small values of $F_9(LUMO+2)^*$ and with negative values of the net charge of atom 11. Atom 11 is a carbon located in ring A and bonded to the N atom linking rings A and B (Fig. 2). The net charge of this atom is positive in all molecules. We need to lower this charge to have a better activity. This can be done, for example, by attaching an electron-donor group to atoms 12, 13 and/or 15 (Fig. 2).

Atom 12 is a carbon located in ring A and bonded to atom 11 (Fig. 2). Table 7 shows that $HOMO_{12}^*$ has a π character in all molecules. Small (negative) values for $S_{12}^E(HOMO)^*$ can be obtained by diminishing the electronic density of this MO at atom 12, making more negative the energy of the MO or by both procedures simultaneously. Also, another possibility is changing the actual $HOMO_{12}^*$ by an inner molecular MO. All these changes transform atom 12 in a bad electron donor. An electron-attractor group at positions 14 and/or 16 would subtract electrons from atom 12. Note that the conditions deduced for atom 12 are contradictory with a negative net charge on atom 11. Now, looking to Table 4 we may see that $S_{12}^E(HOMO)^*$ is the most important variable in Eq. 2 and Q_{11} the less important one. Therefore, we may discard or the moment the conditions for atom 11 waiting for the appearance of new data of new derivatives. Therefore, atom 12 seems to behave a good electron acceptor. Atom 3 is a carbon in ring B and bonded to the N atom linking rings A and B (Fig. 2). Table 6 shows that $S_3^E(HOMO-2)^*$ has a π or σ character following the molecule. A high activity is associated with small (negative) values for $S_3^E(HOMO-2)^*$. Small values are obtained in the same way than we used for $HOMO_{12}^*$. We have analyzed also the plots (not shown here) of $\log(IC_{50})$ *vs.* $S_3^E(HOMO-1)^*$ and $\log(IC_{50})$ vs. $S_3^E(HOMO)^*$. The plot of $\log(IC50)$ *vs.* $S_3^E(HOMO-1)^*$ shows that high activity is associated with low (negative) values for this index. But the plot of $\log(IC_{50})$ *vs.* $S_3^E(HOMO)^*$ shows an opposite trend: a high activity is associated with high (negative) values of $S_3^E(HOMO)^*$. Therefore, atom 3 behaves as an electron-acceptor. Atom 9 is nitrogen in ring C (Fig. 2). A high inhibitory activity is associated with small values of $F_9(LUMO+2)^*$. Table 6 shows that the three lowest empty local MOs of this atom have a π character. The plots of $F_9(LUMO+1)^*$ *vs.* $\log(IC_{50})$ and $F_9(LUMO)^*$ *vs.* $\log(IC_{50})$ (not shown here) shows the same trend. On the other hand, $(HOMO)_9^*$ has a π character in all molecules (Table 6). On this basis we suggest that atom 9 is acting as an electron donor. All the suggestions are displayed in the partial 2D pharmacophore of Fig. 7.
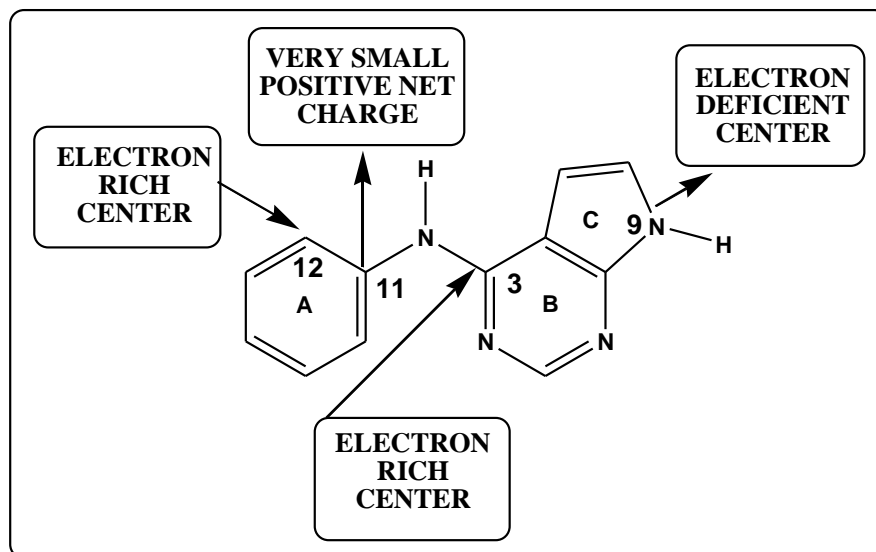
Figure 7: Partial 2D pharmacophore for the inhibition of epidermal growth factor receptor kinase A by a set of N^4-phenyl substituted-7H-pyrrolo[2,3-d]pyrimidin-4-amines

In summary, we have obtained statistically significant relationships between the variation of the inhibitory capacity of a group of N^4-phenylsubstituted-7*H*-pyrrolo[2,3-*d*]pyrimidin-4-amines against aurora kinase A and epidermal growth factor receptor kinase and the variation of the values of several local atomic reactivity indices of some atoms belonging to a common skeleton. These results are depicted in the corresponding partial pharmacophore that could be useful in the design of new and more powerful molecules.

References

[1]. Borisa, A. C.; Bhatt, H. G. A comprehensive review on Aurora kinase: Small molecule inhibitors and clinical trial studies. *European Journal Medicinal Chemistry* 2017, 140, 1-19.

[2]. Kurup, S.; McAllister, B.; Liskova, P.; Mistry, T.; Fanizza, A.; Stanford, D.; Slawska, J.; Keller, U.; Hoellein, A. Design, synthesis and biological activity of N^4-phenylsubstituted-7 *H*-pyrrolo [2, 3-*d*] pyrimidin-4-amines as dual inhibitors of aurora kinase A and epidermal growth factor receptor kinase. *Journal of enzyme inhibition and medicinal chemistry* 2018, 33, 74-84.

[3]. Thirumurugan, K.; Lakshmanan, S.; Govindaraj, D.; Prabu, D. S. D.; Ramalakshmi, N.; Antony, S. A. Design, synthesis and anti-inflammatory activity of pyrimidine scaffold benzamide derivatives as epidermal growth factor receptor tyrosine kinase inhibitors. *Journal of Molecular Structure* 2018, 1171, 541-550.

[4]. Park, H.; Jung, H.Y.; Mah, S.; Hong, S. Systematic Computational Design and Identification of Low Picomolar Inhibitors of Aurora Kinase A. *Journal of chemical information and modeling* 2018, 58, 700-709.

[5]. Mahernia, S.; Hassanzadeh, M.; Sharifi, N.; Mehravi, B.; Paytam, F.; Adib, M.; Amanlou, M. Structure-based pharmacophore design and virtual screening for novel potential inhibitors of epidermal growth factor receptor as an approach to breast cancer chemotherapy. *Molecular diversity* 2018, 22, 173-181.

[6]. Long, L.; Wang, Y.H.; Zhuo, J.X.; Tu, Z.C.; Wu, R.; Yan, M.; Liu, Q.; Lu, G. Structure-based drug design: Synthesis and biological evaluation of quinazolin-4-amine derivatives as selective Aurora A kinase inhibitors. *European journal of medicinal chemistry* 2018, 157, 1361-1375.

[7]. Haghighijoo, Z.; Rezaei, Z.; Jaberipoor, M.; Taheri, S.; Jani, M.; Khabnadideh, S. Structure based design and anti-breast cancer evaluation of some novel 4-anilinoquinazoline derivatives as potential epidermal growth factor receptor inhibitors. *Research in pharmaceutical sciences* 2018, 13, 360.

[8].   Tomassi, S.; Lategahn, J.; Engel, J.; Keul, M.; Tumbrink, H. L.; Ketzer, J.; Muhlenberg, T.; Baumann, M.; Schultz-Fademrecht, C.; Bauer, S.; Rauh, D. Indazole-Based Covalent Inhibitors To Target Drug-Resistant Epidermal Growth Factor Receptor. *Journal of Medicinal Chemistry* 2017, 60, 2361-2372.

[9].   Srivastava, J. K.; Pillai, G. G.; Bhat, H. R.; Verma, A.; Singh, U. P. Design and discovery of novel monastrol-1, 3, 5-triazines as potent anti-breast cancer agent via attenuating Epidermal Growth Factor Receptor tyrosine kinase. *Scientific Reports* 2017, 7, 5851.

[10]. Kong, Y.; Bender, A.; Yan, A. Identification of Novel Aurora Kinase A (AURKA) Inhibitors via Hierarchical Ligand-Based Virtual Screening. *Journal of chemical information and modeling* 2017, 58, 36-47.

[11]. Joshi, G.; Nayyar, H.; Kalra, S.; Sharma, P.; Munshi, A.; Singh, S.; Kumar, R. Pyrimidine containing epidermal growth factor receptor kinase inhibitors: Synthesis and biological evaluation. *Chemical biology & drug design* 2017, 90, 995-1006.

[12]. Hamed, M. M.; Darwish, S. S.; Herrmann, J.; Abadi, A. H.; Engel, M. First bispecific inhibitors of the epidermal growth factor receptor kinase and the NF-κB activity as novel anticancer agents. *Journal of medicinal chemistry* 2017, 60, 2853-2868.

[13]. Sheikh, I. A.; Hassan, H. M. A. In silico identification of novel erlotinib analogues against epidermal growth factor receptor. *Anticancer research* 2016, 36, 6125-6132.

[14]. Lomov, D.; Lyashchuk, S.; Abramyants, M. Design and synthesis of imidazo [4, 5-c] pyridine derivatives as promising Aurora kinase A (AURKA) inhibitors. *Russian Journal of Organic Chemistry* 2016, 52, 1822-1829.

[15]. Gómez-Jeria, J. S. A New Set of Local Reactivity Indices within the Hartree-Fock-Roothaan and Density Functional Theory Frameworks. *Canadian Chemical Transactions* 2013, 1, 25-55.

[16]. Gómez-Jeria, J. S. *Elements of Molecular Electronic Pharmacology (in Spanish)*. 1st ed.; Ediciones Sokar: Santiago de Chile, 2013; p 104.

[17]. Bruna-Larenas, T.; Gómez-Jeria, J. S. A DFT and Semiempirical Model-Based Study of Opioid Receptor Affinity and Selectivity in a Group of Molecules with a Morphine Structural Core. *International Journal of Medicinal Chemistry* 2012, 2012 Article ID 682495, 1-16.

[18]. Gómez-Jeria, J. S.; Ojeda-Vergara, M. Parametrization of the orientational effects in the drug-receptor interaction. *Journal of the Chilean Chemical Society* 2003, 48, 119-124.

[19]. Gómez-Jeria, J. S. Modeling the Drug-Receptor Interaction in Quantum Pharmacology. In *Molecules in Physics, Chemistry, and Biology*, Maruani, J., Ed. Springer Netherlands: 1989; Vol. 4, pp 215-231.

[20]. Gómez-Jeria, J. S. On some problems in quantum pharmacology I. The partition functions. *International Journal of Quantum Chemistry* 1983, 23, 1969-1972.

[21]. Peradejordi, F.; Martin, A. N.; Cammarata, A. Quantum chemical approach to structure-activity relationships of tetracycline antibiotics. *Journal of Pharmaceutical Sciences* 1971, 60, 576-582.

[22]. Gómez-Jeria, J. S. Tables of proposed values for the Orientational Parameter of the Substituent. I. Monoatomic, Diatomic, Triatomic, n-C_nH_{2n+1}, O-n-C_nH_{2n+1}, NRR', and Cycloalkanes (with a single ring) substituents. *Research Journal of Pharmaceutical, Biological and Chemical Sciences* 2016, 7, 288-294.

[23]. Gómez-Jeria, J. S.; Ojeda-Vergara, M.; Donoso-Espinoza, C. Quantum-chemical Structure-Activity Relationships in carbamate insecticides. *Molecular Engineering* 1995, 5, 391-401.

[24]. Gómez-Jeria, J. S.; Kpotin, G. Some Remarks on The Interpretation of The Local Atomic Reactivity Indices Within the Klopman-Peradejordi-Gómez (KPG) Method. I. Theoretical Analysis. *Research Journal of Pharmaceutical, Biological and Chemical Sciences* 2018, 9, 550-561.

[25]. Gómez-Jeria, J. S. 45 Years of the KPG Method: A Tribute to Federico Peradejordi. *Journal of Computational Methods in Molecular Design* 2017, 7, 17-37.

[26]. Leal, M. S.; Robles-Navarro, A.; Gómez-Jeria, J. S. A Density Functional Study of the Inhibition of Microsomal Prostaglandin E2 Synthase-1 by 2-aryl substituted quinazolin-4(3*H*)-one, pyrido[4,3-

d]pyrimidin-4(3*H*)-one and pyrido[2,3-*d*]pyrimidin-4(3*H*)-one derivatives. *Der Pharmacia Lettre* 2015, 7, 54-66.

[27]. Gómez-Jeria, J. S.; Valdebenito-Gamboa, J. A Density Functional Study of the Relationships between Electronic Structure and Dopamine D_2 receptor binding affinity of a series of [4-(4-Carboxamidobutyl)]-1-arylpiperazines. *Research Journal of Pharmaceutical, Biological and Chemical Sciences* 2015, 6, 203-218.

[28]. Gómez-Jeria, J. S.; Valdebenito-Gamboa, J. Electronic structure and docking studies of the Dopamine D_3 receptor binding affinity of a series of [4-(4-Carboxamidobutyl)]-1-arylpiperazines. *Der Pharma Chemica* 2015, 7, 323-347.

[29]. Gómez-Jeria, J. S.; Robles-Navarro, A. A Quantum Chemical Study of the Relationships between Electronic Structure and cloned rat $5\text{-}HT_{2C}$ Receptor Binding Affinity in N-Benzylphenethylamines. *Research Journal of Pharmaceutical, Biological and Chemical Sciences* 2015, 6, 1358-1373.

[30]. Gómez-Jeria, J. S.; Robles-Navarro, A. DFT and Docking Studies of the Relationships between Electronic Structure and $5\text{-}HT_{2A}$ Receptor Binding Affinity in N-Benzylphenethylamines. *Research Journal of Pharmaceutical, Biological and Chemical Sciences* 2015, 6, 1811-1841.

[31]. Gómez-Jeria, J. S.; Robles-Navarro, A. A Quantum Chemical Analysis of the Inactivation Rate Constant of the BoNT/A LC Neurotoxin by some 1,4-Benzoquinone and 1,4-Naphthoquinone derivatives. *Journal of Computational Methods in Molecular Design* 2015, 5, 15-26.

[32]. Gómez-Jeria, J. S. A DFT study of the relationships between electronic structure and peripheral benzodiazepine receptor affinity in a group of N,N-dialkyl-2- phenylindol-3-ylglyoxylamides (Erratum in: J. Chil. Chem. Soc., 55, 4, IX, 2010). *Journal of the Chilean Chemical Society* 2010, 55, 381-384.

[33]. Gómez-Jeria, J. S.; Soto-Morales, F.; Rivas, J.; Sotomayor, A. A theoretical structure-affinity relationship study of some cannabinoid derivatives. *Journal of the Chilean Chemical Society* 2008, 53, 1393-1399.

[34]. Gómez-Jeria, J. S.; Gerli-Candia, L. A.; Hurtado, S. M. A structure-affinity study of the opioid binding of some 3-substituted morphinans. *Journal of the Chilean Chemical Society* 2004, 49, 307-312.

[35]. Gómez-Jeria, J. S.; Soto-Morales, F.; Larenas-Gutierrez, G. A Zindo/1 Study of the Cannabinoid-Mediated Inhibition of Adenylyl Cyclase. *Iranian International Journal of Science* 2003, 4, 151-164.

[36]. Gómez-Jeria, J. S.; Lagos-Arancibia, L. Quantum-chemical structure-affinity studies on kynurenic acid derivatives as Gly/NMDA receptor ligands. *International Journal of Quantum Chemistry* 1999, 71, 505-511.

[37]. Gómez-Jeria, J. S.; Morales-Lagos, D.; Rodriguez-Gatica, J. I.; Saavedra-Aguilar, J. C. Quantum-chemical study of the relation between electronic structure and pA2 in a series of 5-substituted tryptamines. *International Journal of Quantum Chemistry* 1985, 28, 421-428.

[38]. Gómez-Jeria, J. S.; Morales-Lagos, D. R. Quantum chemical approach to the relationship between molecular structure and serotonin receptor binding affinity. *Journal of Pharmaceutical Sciences* 1984, 73, 1725-1728.

[39]. Gómez-Jeria, J. S.; Morales-Lagos, D. The mode of binding of phenylalkylamines to the Serotonergic Receptor. In *QSAR in design of Bioactive Drugs*, Kuchar, M., Ed. Prous, J.R.: Barcelona, Spain, 1984; pp 145-173.

[40]. Robles-Navarro, A.; Gómez-Jeria, J. S. A Quantum-Chemical Analysis of the Relationships between Electronic Structure and Citotoxixity, GyrB inhibition, DNA Supercoiling inhibition and anti-tubercular activity of a series of quinoline–aminopiperidine hybrid analogues. *Der Pharma Chemica* 2016, 8, 417-440.

[41]. Gómez-Jeria, J. S.; Sánchez-Jara, B. An introductory theoretical investigation of the relationships between electronic structure and A1, A2A and A3 adenosine receptor affinities of a series of N6-8,9-trisubstituted purine derivatives. *Chemistry Research Journal* 2019, 4, 46-59.

[42]. Gómez-Jeria, J. S.; Gatica-Díaz, N. A preliminary quantum chemical analysis of the relationships between electronic structure and $5\text{-}HT_{1A}$ and $5\text{-}HT_{2A}$ receptor affinity in a series of 8-acetyl-7-hydroxy-4-methylcoumarin derivatives. *Chemistry Research Journal* 2019, 4, 85-100.

[43]. Gómez-Jeria, J. S.; Garrido-Sáez, N. A DFT analysis of the relationships between electronic structure and affinity for dopamine D_2, D_3 and D_4 receptor subtypes in a group of 77-LH-28-1 derivatives. *Chemistry Research Journal* 2019, 4, 30-42.

[44]. Gómez-Jeria, J. S.; Valdebenito-Gamboa, J. A quantum-chemical analysis of the antiproliferative activity of N-3-benzimidazolephenylbisamide derivatives against MGC803, HT29, MKN45 and SW620 cancer cell lines. *Der Pharma Chemica* 2015, 7, 103-121.

[45]. Gómez-Jeria, J. S.; Robles-Navarro, A. Quantum-chemical study of the cytotoxic activity of pyrimidine–benzimidazol hybrids against MCF-7, MGC-803, EC-9706 and SMMC-7721 human cancer cell lines. *Research Journal of Pharmaceutical, Biological and Chemical Sciences* 2015, 6, 755-783.

[46]. Gómez-Jeria, J. S.; Robles-Navarro, A. A theoretical study of the relationships between electronic structure and inhibition of tumor necrosis factor by cyclopentenone oximes. *Research Journal of Pharmaceutical, Biological and Chemical Sciences* 2015, 6, 1337-1351.

[47]. Gómez-Jeria, J. S.; Becerra-Ruiz, M. B. A Preliminary Quantum-Chemical Study of the anti-HIV-1 III_B Activity of a series of Etravirine-VRX-480773 Hybrids. *Der Pharma Chemica* 2015, 7, 362-369.

[48]. Pino-Ramírez, D. I.; Gómez-Jeria, J. S. A Quantum-chemical study of the in vitro cytotoxicity of a series of (Z)-1-aryl-3-arylamino-2-propen-1-ones against human tumor DU145 and K562 cell lines. *American Chemical Science Journal* 2014, 4, 554-575.

[49]. Muñoz-Gacitúa, D.; Gómez-Jeria, J. S. Quantum-chemical study of the relationships between electronic structure and anti influenza activity. 2. The inhibition by 1H-1,2,3-triazole-4-carboxamide derivatives of the cytopathic effects produced by the influenza A/WSN/33 (H1N1) and A/HK/8/68 (H3N2) strains in MDCK cells. *Journal of Computational Methods in Molecular Design* 2014, 4, 48-63.

[50]. Muñoz-Gacitúa, D.; Gómez-Jeria, J. S. Quantum-chemical study of the relationships between electronic structure and anti influenza activity. 1. The inhibition of cytophatic effects produced by the influenza A/Guangdong Luohu/219/2006 (H1N1) strain in MDCK cells by substituted bisaryl amide compounds. *Journal of Computational Methods in Molecular Design* 2014, 4, 33-47.

[51]. Gómez-Jeria, J. S. A Density Functional Study of the Inhibition of the Anthrax Lethal Factor Toxin by Quinoline-based small Molecules related to Aminoquinuride (NSC 12155). *Research Journal of Pharmaceutical, Biological and Chemical Sciences* 2014, 5, 780-792.

[52]. Gómez-Jeria, J. S. A Preliminary Formal Quantitative Structure-Activity Relationship Study of some 1,7-Bis-(amino alkyl)diazachrysene Derivatives as Inhibitors of Botulinum Neurotoxin Serotype A Light Chain and Three P. falciparum Malaria Strains. *Journal of Computational Methods in Molecular Design* 2014, 4, 32-44.

[53]. Gómez-Jeria, J. S. Toward Understanding the Inhibition of Vesicular Stomatitis Virus Replication in MDCK Cells by 4-Quinolinecarboxylic acid Analogues. A Density Functional Study. *Der Pharma Chemica* 2014, 6, 64-77.

[54]. Reyes-Díaz, I.; Gómez-Jeria, J. S. Quantum-chemical modeling of the hepatitis C virus replicon inhibitory potency and cytotoxicity of some pyrido[2,3-d]pyrimidine analogues. *Journal of Computational Methods in Molecular Design* 2013, 3, 11-21.

[55]. Paz de la Vega, A.; Alarcón, D. A.; Gómez-Jeria, J. S. Quantum Chemical Study of the Relationships between Electronic Structure and Pharmacokinetic Profile, Inhibitory Strength toward Hepatitis C virus NS5B Polymerase and HCV replicons of indole-based compounds. *Journal of the Chilean Chemical Society* 2013, 58, 1842-1851.

[56]. Gómez-Jeria, J. S.; Flores-Catalán, M. Quantum-chemical modeling of the relationships between molecular structure and in vitro multi-step, multimechanistic drug effects. HIV-1 replication inhibition and inhibition of cell proliferation as examples. *Canadian Chemical Transactions* 2013, 1, 215-237.

[57]. Barahona-Urbina, C.; Nuñez-Gonzalez, S.; Gómez-Jeria, J. S. Model-based quantum-chemical study of the uptake of some polychlorinated pollutant compounds by Zucchini subspecies. *Journal of the Chilean Chemical Society* 2012, 57, 1497-1503.

[58]. Kpotin, G. A.; Bédé, A. L.; Houngue-Kpota, A.; Anatovi, W.; Kuevi, U. A.; Atohoun, G. S.; Mensah, J.-B.; Gómez-Jeria, J. S.; Badawi, M. Relationship between electronic structures and antiplasmodial activities of xanthone derivatives: a 2D-QSAR approach. *Structural Chemistry* 2019, https://doi.org/10.1007/s11224-019-01333-w.

[59]. Kpotin, G.; Gómez-Jeria, J. S. Quantum-Chemical Study of the Relationships between Electronic Structure and Anti-Proliferative Activities of Quinoxaline Derivatives on the K562 and MCF-7 Cell Lines. *Chemistry Research Journal* 2018, 3, 20-33.

[60]. Kpotin, G.; Gómez-Jeria, J. S. A Quantum-chemical Study of the Relationships Between Electronic Structure and Anti-proliferative Activity of Quinoxaline Derivatives on the HeLa Cell Line. *International Journal of Computational and Theoretical Chemistry* 2017, 5, 59-68.

[61]. Gómez-Jeria, J. S.; Castro-Latorre, P.; Kpotin, G. Quantum Chemical Study of the Relationships between Electronic Structure and Antiviral Activities against Influenza A H1N1, Enterovirus 71 and Coxsackie B3 viruses of some Pyrazine-1,3-thiazine Hybrid Analogues. *International Journal of Research in Applied, Natural and Social Sciences* 2017, 5, 49-64.

[62]. Note. The results presented here are obtained from what is now a routinary procedure. For this reason, we built a general model for the paper's structure. This model contains *standard* phrases for the presentation of the methods, calculations and results because they do not need to be rewritten repeatedly and the number of possible variations to use is finite. In 2019.

[63]. Frisch, M. J.; Trucks, G. W.; Schlegel, H. B.; Scuseria, G. E.; Robb, M. A.; Cheeseman, J. R.; Montgomery, J., J.A.; Vreven, T.; Kudin, K. N.; Burant, J. C.; Millam, J. M.; Iyengar, S. S.; Tomasi, J.; Barone, V.; Mennucci, B.; Cossi, M.; Scalmani, G.; Rega, N. *G03 Rev. E.01*, Gaussian: Pittsburgh, PA, USA, 2007.

[64]. Gómez-Jeria, J. S. *D-Cent-QSAR: A program to generate Local Atomic Reactivity Indices from Gaussian 03 log files. v. 1.0*, v. 1.0; Santiago, Chile, 2014.

[65]. Mulliken, R. S. Electronic Population Analysis on LCAO–MO Molecular Wave Functions. I. *The Journal of Chemical Physics* 1955, 23, 1833-1840.

[66]. Gómez-Jeria, J. S. An empirical way to correct some drawbacks of Mulliken Population Analysis (Erratum in: J. Chil. Chem. Soc., 55, 4, IX, 2010). *Journal of the Chilean Chemical Society* 2009, 54, 482-485.

[67]. Gómez-Jeria, J. S. *STERIC: A program for calculating the Orientational Parameters of the substituents* 2.0; Santiago, Chile, 2015.

[68]. Statsoft. *Statistica v. 8.0*, 2300 East 14 th St. Tulsa, OK 74104, USA, 1984-2007.